

# Enhanced confinement with increased extent of the low magnetic shear region in tokamak plasmas

**Lorenzo Nasi, Marie-Christine Firpo**

Laboratoire de Physique et Technologie des Plasmas (CNRS UMR 7648), Ecole Polytechnique, 91128 Palaiseau cedex, France

E-mail: firpo@lptp.polytechnique.fr

**Abstract.** The Hamiltonian representation of magnetic field lines enables to study their confinement properties in tokamaks through the use of symplectic maps such as the symmetric tokamap and its bounded version, the latter being introduced here. In this time-independent purely magnetic framework, we observed the drastic improvement on the confinement of magnetic field lines produced by the local vanishing of the shear profile. This amounts to a non-twist condition that notably acts in the same way the safety profile being (non-strictly) monotonic or having reversed-shear. We single out the effect of the amount of flatness of the safety profile in the vicinity of its zero shear point. All other things being equal, the beneficial effect of the vanishing of the shear profile is shown to be increased if the radial extent of the low-shear region is increased. To be specific, the low-shear region induces the formation of a belt of robust KAM tori acting as an internal transport barrier whose width is all the larger as the extent of the low-shear region is broad.

PACS numbers: 52.55.Fa, 05.45.+a, 52.25.Gj

Submitted to: *Plasma Physics and Controlled Fusion*

## 1. Introduction

In order to approach ignition, it is required that the present hot tokamak plasmas have a better energy confinement. The energy confinement time is commonly limited by deleterious small-scale turbulent transport. Because internal transport barriers (ITB) [1, 2, 3] reduce or even quench the turbulent transport within the inner plasma region improving energy confinement in the plasma core which should yield high fusion gains, they have become an essential ingredient of advanced scenarios in which the tokamak could operate as an economic steady-state fusion reactor.

The physics of the triggering and sustainment of ITB as well as the explanation of their very nature are still subjects of intensive investigations [3]. Besides an increasingly detailed empirical and experimental knowledge, their theoretical modeling is still incomplete. It is commonly admitted that two ingredients should control their formation, namely the  $\mathbf{E} \times \mathbf{B}$  flow shear and the magnetic shear through the safety factor ( $q$ ) profile. An increased number of works have recently reported the importance of the  $q$ -profile. In particular, Eriksson et al. [4] demonstrated experimentally in the JET tokamak the critical role of the safety factor profile in the formation of ITB by using it as a control parameter in discharges where other parameters, including the  $\mathbf{E} \times \mathbf{B}$  flows, were kept the same. They obtained an ITB for a non-monotonic  $q$  profile (i.e. with reversed shear) but not with a monotone  $q$ . Actually these reversed shear scenarios have been recognized as favorable experimental conditions to obtain ITB whereas the ITB's locations have been mostly related to the low shear zones.

In this article, we wish to study the appearance and robustness of ITB within a purely magnetic and static (time-independent) framework following a line of approach notably initiated by Balescu and coworkers. This simplified, yet relevant, approach is guided by the fact that, in a first approximation, charged particles in a tokamak follow the magnetic field lines so that transport properties for the later transfer to the formers. We shall focus on the influence of the behaviour of the  $q$ -profile in the vicinity of its vanishing shear region on the appearance and robustness of ITB. To be more specific, we wish to single out the role and importance of the amount of *flatness* of the  $q$ -profile in the vicinity of its minimum (for the reversed shear case) or in the vicinity of its inflexion point (in the case of a non-strictly monotonic profile).

In Section 2, the Hamiltonian formulation of magnetic field lines is recalled and symplectic maps are introduced. In order to capture more accurately the magnetic field lines, we shall implement the symmetric tokamap and its bounded version, instead of the standard tokamap. In Section 3, we shall study numerically the influence of the flatness of the  $q$ -profile, in the vicinity of a given inflexion or minimum point, on the overall magnetic field lines stochasticity. To do so, we shall consider a family of polynomial winding number profiles. In Section 4, we eventually consider a sample of tokamak-oriented realistic  $q$ -profiles with reversed shear. This brings another evidence on the favorable role played by an increased extension of the low-shear region around the minimum of the  $q$ -profile. We conclude in Section 5.

## 2. Hamiltonian formulation for magnetic field lines and maps

### 2.1. Hamiltonian framework

In order to investigate the role of the  $q$ -profile on the existence and robustness of ITBs, we shall use the Hamiltonian structure of the magnetic field lines. We shall use in the following traditional generalized toroidal coordinates  $\psi, \theta, \zeta$  where  $\psi$  is the flux coordinate (so that  $\psi = 0$  and  $\psi = 1$  correspond to the magnetic axis and to the plasma boundary, respectively),  $\theta$  is the poloidal angle and  $\zeta$  the toroidal angle. From Maxwell's equation  $\nabla \cdot \mathbf{B} = 0$ , the "equations of motion" for magnetic field lines [5] in a tokamak are

$$\frac{d\psi}{d\zeta} = -\frac{\partial F}{\partial \theta}, \quad \frac{d\theta}{d\zeta} = \frac{\partial F}{\partial \psi} \quad (1)$$

where  $F(\psi, \theta, \zeta)$  is the poloidal flux. Equations (1) have a Hamiltonian structure: the toroidal angle  $\zeta$  plays the role of "time",  $F$  is the Hamiltonian and  $\theta$  and  $\psi$  are canonically conjugated coordinates. In order to consider perturbations from the ideal i.e. integrable case, where  $F = F_0(\psi)$  and magnetic surfaces are nested tori wound around the magnetic axis, let us introduce a stochasticity parameter,  $K$ , such that the Hamiltonian  $F$  is given by the sum of an unperturbed term  $F_0$  and a perturbation  $\delta F(\psi, \theta, \zeta)$  :

$$F = F_0(\psi) + K\delta F(\psi, \theta, \zeta). \quad (2)$$

As  $K$  increases, magnetic surfaces may no longer exist and the problem of their existence is formally equivalent to that of the integrability of a Hamiltonian with one-and-a-half degrees of freedom. In realistic tokamaks, these magnetic perturbations may result e.g. from coil imperfections and/or internal instabilities (tearing). Within the above formalism, the safety factor  $q(\psi)$  is simply related to the unperturbed Hamiltonian since  $q(\psi) = 1/W(\psi)$  where  $W(\psi) \equiv dF_0/d\psi$  is the winding number. Therefore  $q(\psi)$ , the ratio of the number of toroidal turns per poloidal turn, is the inverse of the unperturbed Hamiltonian. Moreover,  $s = d \ln q / d \ln \psi$  is the shear profile.

### 2.2. Maps

**2.2.1. Tokamap** Instead of performing a time consuming integration of the field line differential equations (1), we shall use a simplified but relevant approach, namely the Poincaré map associated to a given poloidal cross-section [6]. It is defined from the intersection points of a magnetic field line starting at position  $(\psi_0, \theta_0)$  with some given poloidal section  $\zeta = cst$ . The intersection point after  $\nu$  toroidal turns is denoted by  $(\psi_\nu, \theta_\nu)$ . The map we shall be interested in, the *tokamap*, was introduced by Balescu and coworkers [7, 8, 9]. Its implicit form is

$$\psi_{\nu+1} = \psi_\nu - K \frac{\psi_{\nu+1}}{1 + \psi_{\nu+1}} \sin \theta_\nu \quad (3)$$

$$\theta_{\nu+1} = \theta_{\nu} + W(\psi_{\nu+1}) - \frac{K}{2\pi} \frac{1}{(1 + \psi_{\nu+1})^2} \cos \theta_{\nu}.$$

Explicitly, we have

$$\psi_{\nu+1} = \frac{1}{2} \left( P(\psi_{\nu}, \theta_{\nu}) + \sqrt{[P(\psi_{\nu}, \theta_{\nu})]^2 + 4\psi_{\nu}} \right) \quad (4)$$

$$\theta_{\nu+1} = \theta_{\nu} + W(\psi_{\nu+1}) - \frac{K}{2\pi} \frac{1}{(1 + \psi_{\nu+1})^2} \cos \theta_{\nu} \quad (5)$$

where

$$P(\psi, \theta) = \psi - 1 - K \sin \theta. \quad (6)$$

This map is an area-preserving map which is compatible with the toroidal geometry [7] due to the following important physical properties : (i) the toroidal flux  $\psi$  is always positive (this is necessary since  $\psi \sim r^2$  where  $r$  is the minor radius of the tokamak) and (ii) the magnetic axis is invariant ( $\psi = 0$  is mapped to  $\psi = 0$ ). It has proved to be an important model since it correctly describes the qualitative features of the magnetic field lines stochasticity known in tokamak physics.

*2.2.2. Symmetric tokamap* Some studies have recently pointed some limitations of this model. It actually turns out that despite a qualitative agreement with the actual magnetic field behaviour obtained from the continuous Hamiltonian system formed by Eqs. (1) and (2), the tokamap is far less accurate than its symmetric version as proposed by Abdullaev [10, 6]. We shall therefore implement in this study the symmetric tokamap instead of the standard one. The symmetric tokamap very closely describes the continuous Hamiltonian system (2) with

$$K\delta F(\psi, \theta, \zeta) = -\frac{K}{(2\pi)^2} \frac{\psi}{1 + \psi} \sum_{n=-M}^M \cos(\theta - n\zeta), \quad (7)$$

and  $2M + 1 \gg 1$ , from which it is derived. Its implicit form is given by

$$\begin{aligned} \Psi_{\nu} &= \psi_{\nu} - \frac{K}{2\pi} \frac{\Psi_{\nu}}{1 + \psi_{\nu}} \sin \theta_{\nu} \\ \Theta_{\nu} &= \theta_{\nu} - \frac{K}{2\pi} \frac{1}{(1 + \Psi_{\nu})^2} \cos \theta_{\nu} \\ \Theta_{\nu+1} &= \Theta_{\nu} + 2\pi W(\Psi_{\nu}) \\ \Psi_{\nu+1} &= \Psi_{\nu} \\ \psi_{\nu+1} &= \Psi_{\nu+1} - \frac{K}{2\pi} \frac{\Psi_{\nu+1}}{1 + \Psi_{\nu+1}} \sin \theta_{\nu+1} \\ \theta_{\nu+1} &= \Theta_{\nu+1} - \frac{K}{2\pi} \frac{1}{(1 + \Psi_{\nu+1})^2} \cos \theta_{\nu+1} \end{aligned} \quad (8)$$

where  $K$  is the stochasticity parameter and the auxiliary variables  $\Theta$  and  $\Psi$  are determined iteratively by the map from a given starting point  $(\theta_0, \psi_0)$ . Contrarily to the tokamap, a numerical approximation is necessary in order to solve the last equation of the symmetric tokamap (8) with respect to variable  $\theta_{\nu+1}$ , but this is an affordable task with usual interpolation methods such as Newton's method or the Brent's algorithm [11] that we used here.

*2.2.3. Bounded symmetric tokamap* Another adjustment to the tokamap has also been recently proposed: the bounded tokamap. Whereas the tokamap does not impose any upper boundary limit for  $\psi$ , so that it can be directly used in the ergodic divertor problem [12] where magnetic field lines may go outside the last magnetic surface (defined as  $\psi = 1$ ), its bounded version is constructed by requiring that  $\psi = 1$  cannot be crossed. We used the approach developed in Refs. [13, 14] to propose the symmetric version of the bounded tokamap with

$$K\delta F(\psi, \theta, \zeta) = -\frac{K}{(2\pi)^2}\psi(1-\psi) \sum_{n=-M}^M \cos(\theta - n\zeta) \quad (9)$$

and  $2M + 1 \gg 1$ . This form of perturbation ensures that not only the magnetic axis, corresponding to  $\psi = 0$ , but also the plasma boundary, corresponding to  $\psi = 1$  are invariant under the map and cannot be crossed.

Then, applying the same method [10, 6] as in Sec. 2.2.2, we propose the symmetric version of the bounded tokamak as

$$\begin{aligned} \Psi_\nu &= \psi_\nu - \frac{K}{2\pi}\Psi_\nu(1-\Psi_\nu) \sin \theta_\nu \\ \Theta_\nu &= \theta_\nu - \frac{K}{2\pi}(1-2\Psi_\nu) \cos \theta_\nu \\ \Theta_{\nu+1} &= \Theta_\nu + 2\pi W(\Psi_\nu) \\ \Psi_{\nu+1} &= \Psi_\nu \\ \psi_{\nu+1} &= \Psi_{\nu+1} - \frac{K}{2\pi}\Psi_\nu(1-\Psi_\nu) \sin \theta_{\nu+1} \\ \theta_{\nu+1} &= \Theta_{\nu+1} - \frac{K}{2\pi}(1-2\Psi_\nu) \cos \theta_{\nu+1}. \end{aligned} \quad (10)$$

The first equation of (10) has two roots for  $\Psi_\nu$  and the positive one is retained. This modeling is valid for not too large values of the stochasticity parameter as it is required that  $K/2\pi < 1$ .

### 2.3. Motivations

From the theoretical point of view, the effect of various parameters describing the  $q$ -profile, such as the boundary values of the  $q$ -profile, the value of the minimum of the  $q$ -profile in the reversed shear version (in the so-called rev-tokamap), for Hamiltonian maps have already been considered [15, 16]. Yet, this has been mainly limited to restricted choices of  $q$  profiles. In addition, to the authors' knowledge, an essential point has not been investigated systematically: the effect of the local flatness of the  $q$ -profile on (hopefully) realistic models for magnetic field lines in a tokamak. This is in our sense a crucial point since there is strong experimental evidence that the radial extent of the low shear region of safety factor's profile plays an outstanding role on ITBs' appearance and robustness [17, 2, 3]. Thus, modeling is needed in order to asses one of the "critical physics issues relevant to the extrapolation of ITB regimes to next-step experiments, such as ITER" [18] : the optimum  $q$ -profile. This forms the ultimate perspective of the present work.

### 3. Numerical results on the stochasticity of magnetic field lines for polynomial winding number profiles

We are interested in assessing the influence of the extent of the low shear region on magnetic confinement. Since it happens that the Hamiltonian (2) is more directly linked to the winding number, since  $W(\psi) \equiv dF_0/d\psi$ , than the  $q$ -profile, we shall consider it in the following. We are then particularly interested in the influence of the behaviour of the  $W$ -profile in the vicinity of some unique  $\psi_0$  such that  $W'(\psi_0) = 0$ . If such a  $\psi_0$  exists, the twist condition for the corresponding map is violated, that is the symmetric tokamak is *non-twist*. A straightforward way to study such behaviour is to consider the family of polynomial  $W$ -profiles :

$$W(\psi) = -c(\psi - \psi_0)^n + W_0 \quad (11)$$

where  $n$  is a positive integer representing the degree of degeneracy of the zero  $\psi_0$  of the shear profile ‡ associated to (11). Although there is an extensive bunch of experimental evidence that the maximum value of the winding number influences ITB formation in the reversed shear case [17, 2, 3], this will not be our point here and we shall rather impose here on an arbitrary basis  $W_0 = 5/2\pi$ ,  $c = 1.3$  and  $\psi_0 = 0.5$  in order to focus on the flatness of the  $W$ -profile only.

For every profile (11), with the degree  $n$  going from 1 to 8, the phase portrait of the symmetric tokamak (8) has been computed. The results of this iterative process, for  $\psi$  in the physical domain  $[0, 1]$ , are given for the same value  $K = 3$  of the stochasticity parameter in Fig. 1. Several comments are called for. First of all, it is clear from the figure that the case  $n = 1$  is dramatically different from the others. In the case  $n = 1$ , the map is twist as  $W'(\psi)$  does not vanish. The figure exemplifies the *dramatic improvement on confinement induced by the non-twist condition* that is satisfied when  $n \geq 2$ . This has been discussed recently on a general basis by Rypina *et al.* [19]. Secondly, when the non-twist condition is satisfied, the core magnetic field lines are almost integrable. The central non-chaotic region is all the broader in  $\psi$ -space as the  $W$ -profile is flat around  $\psi_0$ , namely as  $n$  is large. Yet this effect saturates rapidly: for  $n \geq 6$ , the phase space portraits are almost indistinguishable. This is not surprising as the corresponding  $q$ -profiles are indeed almost identical. Thirdly, there is a perfect progression in the phase space appearances between the odd and even  $n$ -exponents as  $n$  increases in the non-twist case i.e. for  $n \geq 2$ . This means that the fact that the  $q$ -profile has a reversed shear or not is not important in terms of the confinement of the magnetic field lines. What matters is the degree of degeneracy of the zero of the shear profile or, so to speak, the amount of local flatness of the  $W$ -profile. To check this explicitly, let us consider the two following profiles

$$W_m(\psi) = -c(\psi - \psi_0)^3 + W_0 \quad (12)$$

$$W_{rs}(\psi) = -c|(\psi - \psi_0)|^3 + W_0 \quad (13)$$

‡ More precisely,  $\psi_0$  is a zero of the shear profile when  $n \geq 2$ .

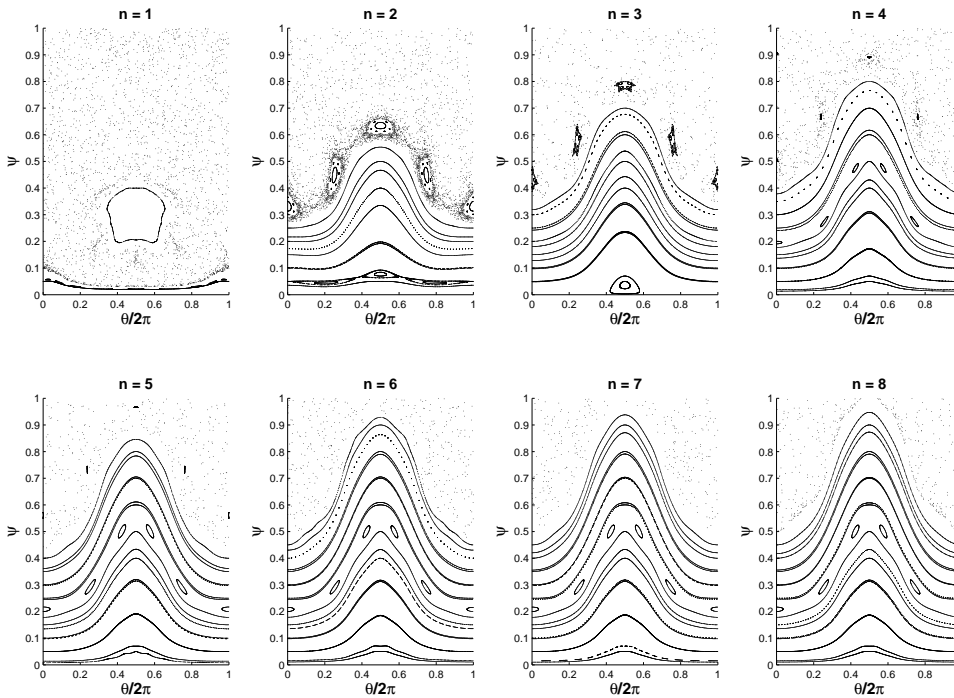


**Figure 1.** Phase space portraits of the symmetric tokamap (8) for different values of the order of degeneracy  $n$  of the profile (11). Parameters are  $K = 3$ ,  $W_0 = 5/2\pi$ ,  $c = 1.3$  and  $\psi_0 = 0.5$ .

where  $W_m$  (12) and  $W_{rs}$  (13) correspond respectively to a monotonic and to a reversed-shear profiles with the same local flatness ( $n = 3$ ). The results are displayed in figure 2. This shows that the global behaviour of the magnetic field lines is indeed the same in both cases: the outer stochastic region is identical. There are only some limited apparent topological discrepancies in the inner ordered zone. This third point is rather novel since previous studies [15] commonly used to focus solely on reversed-shear  $q$ -profiles to get the non-twist condition.

We have brought some numerical evidence of the influence on magnetic confinement of the amount of flatness of the  $q$ -profile around its extremum. In order to definitely ascertain this phenomenon, we eventually wish to avoid the possible bias induced by using different edge values of  $W$  for each  $n$  in Fig. 1. It actually happens that increasing the edge value of a polynomial  $W$ -profile (11) with given degree  $n$  may induce the stochastization of the, otherwise regular, core magnetic field lines. This is illustrated in Fig. 3 for the case  $n = 2$ . Therefore, in order to single out the effect of the flatness of the  $W$ -profile i.e. of the radial extent of the low-shear region around an extremum, the study shown in Fig. 1 was revised for the polynomial profiles (11) with variable  $c = c_n$  such that  $W(0) = W(1)$  be a given constant for all  $n$ . Results are depicted in Fig. 4 for even values of  $n$  between 2 and 8. This figure shows that, *all other things being equal*, the radial extent of the regular magnetic field lines is all the wider as the low shear

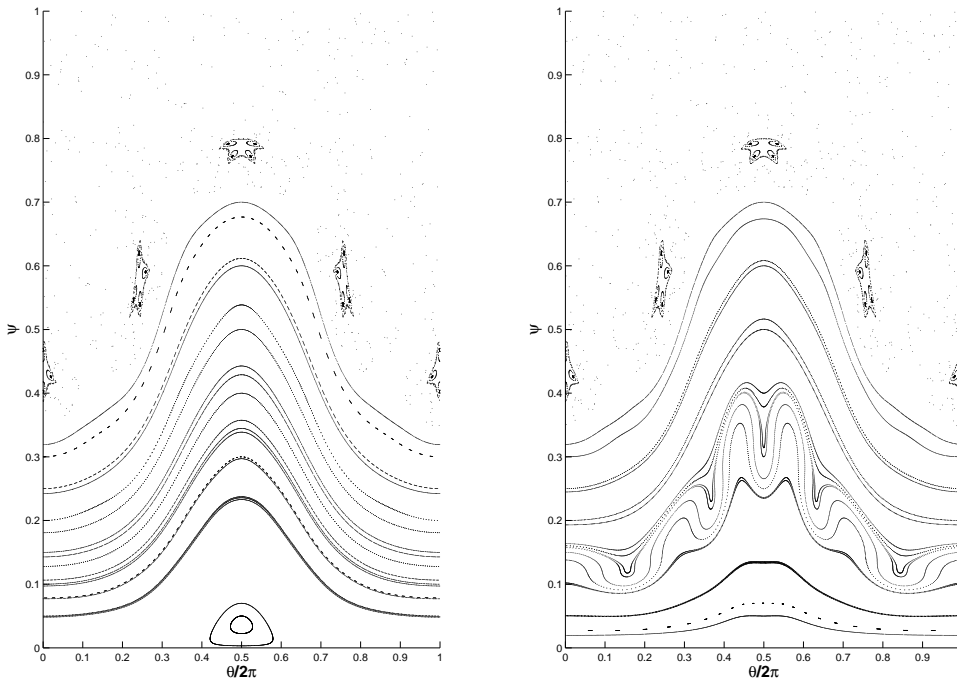


**Figure 2.** Phase space portraits of the symmetric tokamap (8). (left)  $W_m(\psi)$  is given by (12); (right)  $W_{rs}(\psi)$  is given by (13). Parameters  $K = 3$ ,  $W_0 = 5/2\pi$ ,  $c = 1.3$  and  $\psi_0 = 0.5$ .

region around the extremum of the  $q$ -profile is broad.

Finally, we wish to insist on the fact that the above conclusion does not depend on the particular choice of the map. It remains valid when considering the - less accurate - standard tokamap and the bounded version of the symmetric tokamap. In this case, the appearance of internal transport barriers can be seen more easily. This can be shown in Fig. 5. Whereas global chaos can be observed for  $n = 1$ , the non-twist effect that takes places for  $n \geq 2$  dramatically improves confinement. A clear internal transport barrier emerges for  $n = 2$  separating the internal and the outer chaotic regions. Increasing  $n$ , that is the extent of the low shear region, induces a drastic reduction of chaos.

#### 4. Influence of the radial extent of the low-shear region for some realistic reversed shear $q$ -profiles

The previous academic case of polynomial centered  $W$ -profiles is not realistic. We wish in this Section to briefly test our results on the beneficial effect of the increased radial extent of the low shear domain on more experimentally compatible  $q$ -profiles. We shall here consider reversed shear profiles leading to ITBs. Typical locations of the minimum of the  $q$ -profile correspond to a normalized radius of 0.3-0.4 [1] and to a central  $q(0) \simeq 3$  while  $q_{min}$ , the minimum value of  $q$ , is about 2. We have considered three  $q$ -profiles



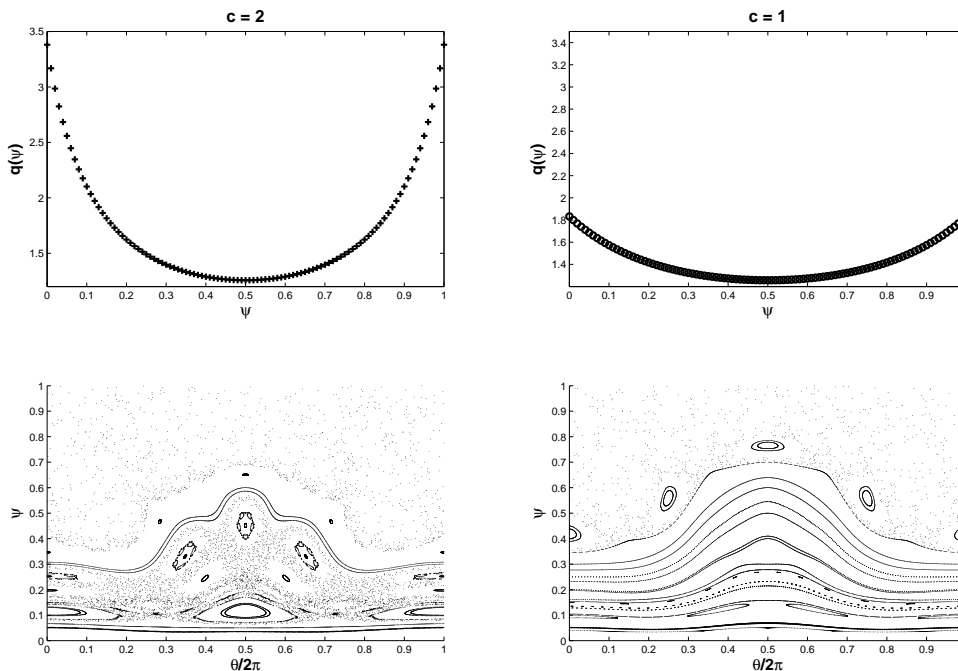


**Figure 3.** Phase space portraits of the symmetric tokamap (8) with  $W(\psi) = 5/2\pi + c(\psi - .5)^2$  and  $K = 3$  for: (left)  $c = 2$ , (right)  $c = 1$ .

compatible with these realistic data and computed the corresponding phase portraits for the magnetic field lines. The results are given in Fig. 6. It is once again clear from this figure that, for increasing flatness of  $q$  about its minimum and for constant  $K$ , the extent of the non-chaotic, regular, magnetic field lines in the plasma core is broader. In order to show that this effect is robust, namely map independent, we have computed the phase space portraits for the symmetric bounded tokamap (10) for the same  $q$ -profiles. Results are plotted in Fig. 6. We do observe once again that for increasing flatness there is chaos reduction.

A quantitative indicator of the degree of flatness of some  $W$ -profile around its extremum located at  $\psi_0$  could be given by  $f_W(\psi_0) \equiv \lim_{\psi \rightarrow \psi_0} \ln |W(\psi) - W(\psi_0)| / \ln |\psi - \psi_0|$ . As shown previously on polynomial profiles, for a given stochasticity parameter, confinement is improved as  $f_W(\psi_0)$  increases. However,  $f_W(\psi_0)$  gives the power of the first non-vanishing term in the Taylor expansion of the  $W$ -profile around  $\psi_0$ . Since realistic reversed-shear profiles are generically approximated locally by a parabola, this would yield  $f_W(\psi_0) = 2$ . This has been checked on the above profiles. It is thus necessary to produce a practical indicator of the local amount of low shear. Let us then assume that the reversed shear profile may be locally Taylor expanded as

$$W(\psi) = W(\psi_0) + \frac{1}{2}W''(\psi_0)\delta\psi^2 + O(\delta\psi^3), \quad (14)$$

with  $\delta\psi \equiv \psi - \psi_0$ . Then, for a given  $W(\psi_0)$ , the local flatness of  $W$  increases as

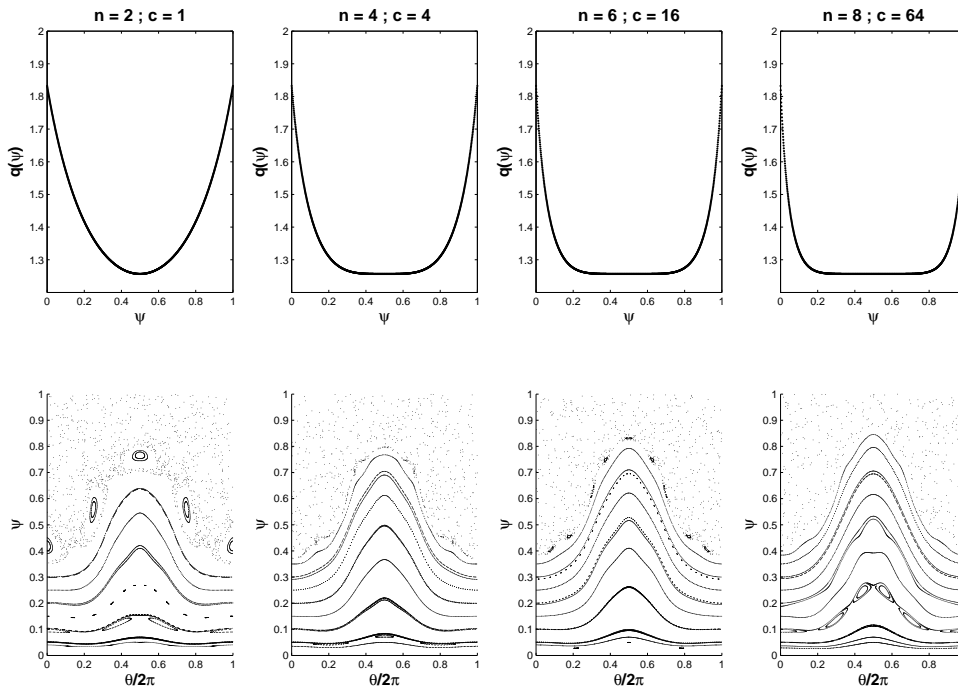


**Figure 4.** (up) Reversed-shear  $q$ -profiles given by  $q(\psi) = 1/[5/2\pi + c_n(\psi - .5)^n]$  with identical boundary values and increasing central flatness (with  $n$  even between 2 and 8) with (down) their corresponding phase space portraits of the symmetric tokamap (8) for  $K = 3$ .

$|W''(\psi_0)|$  becomes smaller. This is in agreement with the results given in Fig. 6 where a diminution of  $W''(\psi_0)$  corresponding to an increased local flatness is observed from left to right. More precisely, one obtains numerically  $W''(\psi_0) = 10.6$  for the profile located at the left of Fig. 6,  $W''(\psi_0) = 7.8$  for the middle profile and  $W''(\psi_0) = 7.4$  for the right one. Finally, let us note that in this Figure as well as in Fig. 5, the stochasticity parameter  $K$ , that is proportional to the relative amount of magnetic perturbation [8], has been taken unrealistically large. This points to the fact that the effect of low shear is much stronger than usual KAM results on the survival of tori that would be obtained for monotone  $q$ -profiles and corresponding twist maps [See e.g. the large scale chaos exhibited in the tokamap phase portrait of Fig. 9 in the work by Misguich et al. [8] that is obtained also for  $K = 6$ ].

## 5. Conclusions

The Hamiltonian formalism has been used to account for the behavior of magnetic field lines under some perturbations of given equilibrium safety factor profiles. The corresponding symplectic maps were the symmetric tokamap and its bounded version in which the last magnetic surface cannot be crossed. In this time-independent framework,

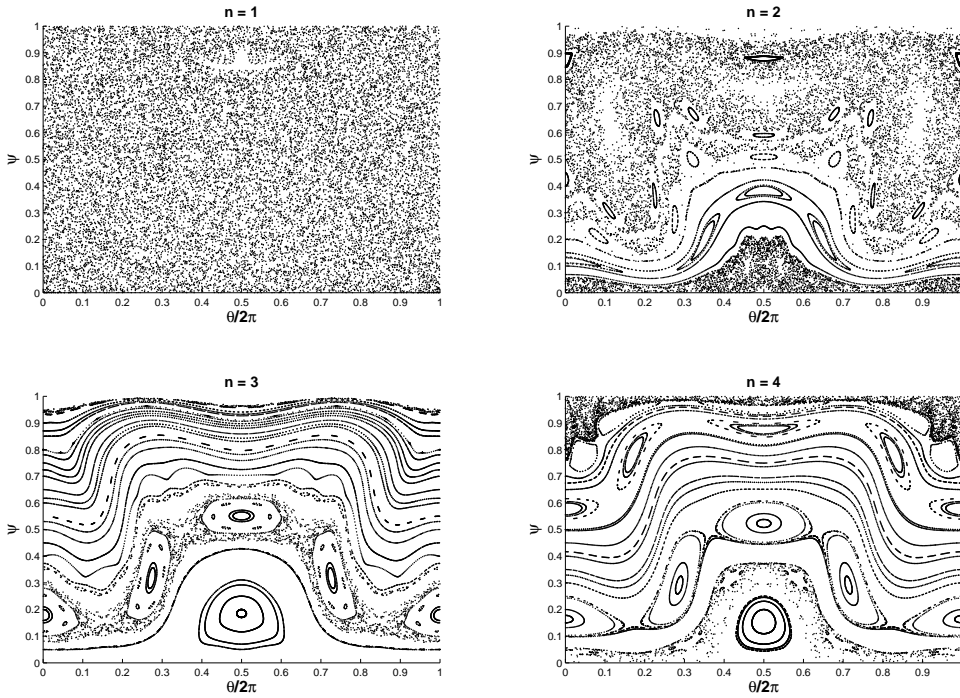


**Figure 5.** Phase space portraits of the bounded symmetric tokamak (10) for different values of the order of degeneracy  $n$  ( $n = 1, 2, 3$  and  $4$ ) of the profile (11). Parameters are  $K = 6$ ,  $W_0 = 5/2\pi$ ,  $c = 1.3$  and  $\psi_0 = 0.5$ .

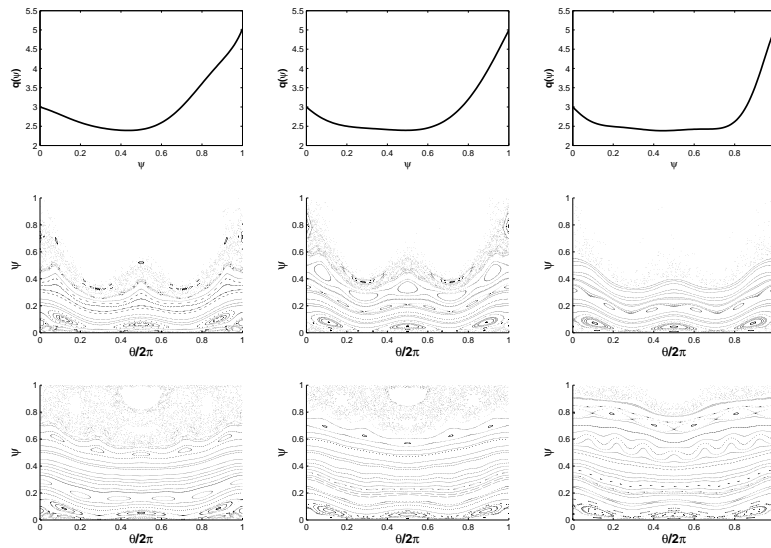


**Figure 6.** (top)  $q$ -profiles of increasing local flatness around  $q_{min}$ ; (middle) corresponding phase space portraits of the symmetric tokamak (8) for 500 iterations and  $K = 6$ ; (bottom) same as above for the bounded symmetric tokamak (10).

we have shown the drastic improvement on the confinement of magnetic field lines produced by the local vanishing of the shear profile: the existence of some  $\psi_0$  such that  $q'(\psi_0) = 0$  is a non-twist condition that acts in the same way the safety profile being monotonic or having reversed-shear. All other things being equal, the beneficial effect of this vanishing of the shear profile was shown to be increased if the radial extent of the low-shear region was increased. To be specific, the low-shear region induces the formation of a belt of robust KAM tori acting as an internal transport barrier whose width is all the larger as the extent of the low-shear region is broad. This conclusion has been derived here without any consideration of dynamical stability. It is important to note that there are additional dynamical arguments that favor a reduction of (electrostatic) turbulence for low magnetic shear, since it is well known that the linear growth rates of drift and ballooning type modes vanish at zero shear [20].

Finally, we wish to conclude by discussing the validity of this simplified purely magnetic approach. An obvious limitation of the model comes from its lack of self-consistency. In particular, there is no retroaction on the turbulence level. However, we would like to stress that such a simplified picture, being in a Hamiltonian form (due to the magnetic field being divergence-free), inherits from robustness properties w.r.t. fluctuations. This is a general property of Hamiltonian systems and ensures that their long-time simulations are valid, at least in an average sense [21]. In the present model, this means that introducing some small perturbation in the symplectic symmetric tokamak, such a perturbation being e.g. a reduction of the magnetic turbulence [22] or another perturbation that may reflect the effect of electrostatic turbulence, the essential features of the model are fully preserved.

It is now desirable to improve the connection of the present results with tokamak experiments and complete the modeling to address thermal transport. This would amount to couple the present magnetic approach to some heat transport modeling. Nevertheless, we believe that the benefits of the purely magnetic approach, initiated notably by Balescu, have not been exhausted yet. The role of the value of the  $q$ -profile in the low shear zone as well as the role of edge-gradients of the  $q$ -profile are other challenging important questions on which we shall be focusing our attention in a shortcoming future.

## Acknowledgments

Fruitful discussions with M. Bécoulet, X. Garbet, P. Hennequin, H. Lütjens and J.-M. Rax are gratefully acknowledged. The authors especially thank G. Steinbrecher for useful communications on tokamak related works.

- [1] R.C. Wolf. Internal transport barriers in tokamak plasmas. *Plasma Phys. Control. Fusion*, 45:R1–R91, 2003.
- [2] J. W. Connor et al. A review of internal transport barriers physics for steady-state operation of tokamaks. *Nucl. Fusion*, 44:R1–R49, 2004.
- [3] T. Tala, X. Garbet, and JET EFDA contributors. Physics of internal transport barriers. *C. R. Physique*, 7:622–633, 2006.
- [4] L.-G. Eriksson, C. Fourment, V. Fuchs, X. Litaudon, C.D. Challis, F. Crisanti, B. Esposito, X. Garbet, C. Giroud, N. Hawkes, P. Maget, D. Mazon, and G. Tresset. Discharges in the jet tokamak where the safety factor profile is identified as the critical factor for triggering internal transport barriers. *Phys. Rev. Lett.*, 88(145001), 2002.
- [5] R. D. Hazeltine and J. D. Meiss. *Plasma Confinement*. Dover, 2003.
- [6] S. S. Abdullaev. *Construction of Mappings for Hamiltonian Systems and Their Applications*. Springer, 2006.
- [7] R. Balescu, M. Vlad, and F. Spineanu. Tokamap : A hamiltonian twist map for magnetic field lines in toroidal geometry. *Phys. Rev. E*, 58(1):951 – 964.
- [8] J.H. Misguich, J.-D. Reuss, D. Constantinescu, G. Steinbrecher, M. Vlad, F. Spineanu, B. Weyssow, and R. Balescu. Noble internal transport barriers and radial subdiffusion of toroidal magnetic lines. *Ann. Phys. Fr.*, 28(6):1–101, 2003.
- [9] B. Weyssow and J.H. Misguich. Hamiltonian map for guiding centres in a perturbed toroidal magnetic geometry. In *Europhysics Conference Abstracts*, volume 23J. 26<sup>th</sup> EPS Conf. on Contr. Fusion and Plasma Physics, 1999.
- [10] S. S. Abdullaev. On mapping models of field lines in a stochastic magnetic field. *Nucl. Fusion*, 44:S12–S27, 2004.
- [11] R.P. Brent. *Algorithms for Minimization Without Derivatives*, chapter 3-4.
- [12] S.S. Abdullaev, K.H. Finken, and K.H. Spatschek. Asymptotical and mapping methods in study of ergodic divertor magnetic field in a toroidal system. *Phys. Plasmas*, 6:153–174, 1999.
- [13] V.N. Kuzovkov and O. Dumbrajs. Bounded tokamap. *Annals of the University of Craiova, Physics AUC.*, 17:86–99, 2007.
- [14] V. N. Kuzovkov and O. Dumbrajs. Bounded tokamap : a hamiltonian map for magnetic field lines in a tokamak. *Comp. Model. New Tech.*, 11(2):18–22, 2007.
- [15] R. Balescu. Hamiltonian nontwist map for magnetic field lines with locally reversed shear in toroidal geometry. *Phys. Rev. E*, 58(3):3781–3792, 1998.
- [16] D. Constantinescu and R. Constantinescu. Transport barriers and diffusion phenomena for the magnetic field lines in tokamak. *Physica Scripta*, T118:244–250, 2005.
- [17] Yu F. Baranov, X. Garbet, N.C. Hawkes, B. Alper, R. Barnsley, C.D. Challis, C. Giroud, E. Joffrin, M. Mantsinen, F. Orsitto, V. Parail, S.E. Sharapov, and the JET EFDA contributors. On the link between the  $q$ -profile and internal transport barriers. *Plasma Phys. Control. Fusion*, 46:1181–1196, 2004.
- [18] X. Litaudon. Internal transport barriers : critical physics issues? *Plasma Phys. Control. Fusion*, 48:A1–A34, 2006.
- [19] I. I. Rypina, M.G. Brown, F. J. Beron-Vera, H. Koçak, M. J. Olascoaga, and I. A. Udovydchenkov. Robust transport barriers resulting from strong kolmogorov-arnold-moser stability. *Phys. Rev. Lett.*, 98(104102), 2007.
- [20] J.W. Connor and R.J. Hastie. Microstability in tokamaks with low magnetic shear. *Plasma Phys. Control. Fusion*, 46:1501–1535, 2004.
- [21] G. Steinbrecher and B. Weyssow. Stability under perturbations of the large time average motion of dynamical systems with conserved phase space volume. *arXiv:math-ph/0511091v1*, 2005.
- [22] X.L. Zou, L. Colas, M. Paume, J.M. Chareau, L. Laurent, P. Devynck, and D. Gresillon. Internal magnetic turbulence measurement in plasma by cross polarization scattering. *Phys. Rev. Lett.*, 75:1090–1093, 1995.